Innov. Infrastruct. Solut. (2017)2:2
DOI 10.1007/s41062-016-0050-7

TECHNICAL PAPER

Seismic resilience of isolated bridge configurations with soil–structure interaction

Davide Forcellini[1]

Received: 27 August 2016 / Accepted: 27 December 2016

Abstract Assessment of failure probabilities is one of the key points to define the seismic resilience (SR) of systems. Evaluation of the most proper countermeasure—such as retrofitting, recovery, or reconstruction—to return to the original functionality is a crucial issue, which has to deal with economic limitations. In this regard, bridges are fundamental for the network serviceability and communities' functionality during earthquakes, and in case of emergencies, their accessibility must be guaranteed. In this background, the paper aims at evaluating SR of a benchmark bridge improving its performance by means of isolation technique. It is based on the application of a performance-based earthquake engineering methodology, by the Pacific Earthquake Engineering Research center. Isolation technique contribution is assessed in terms of costs and time quantities with peak ground velocity levels. These outcomes have been applied to estimate the SR of the bridge and thus proposing an attempt of application to a real case study. Recovery costs and time have been implemented inside the traditional definition of resilience and its calculation has been used to assess different scenarios. The paper can be considered as a reference to evaluate recovery procedures by assessing economic performances. Such approach is fundamental for decision makers, stakeholders, professional engineers, and consultants as well.

Keywords Earthquake · Resilience · Bridge · Isolation · Soil structure interaction

✉ Davide Forcellini
davforc@omniway.sm

[1] Structural Engineering Department, University of San Marino, San Marino, San Marino

Background

Seismic resilience (SR) can be defined as the ability of a system to reduce the chances, to absorb, and to recover after of a natural event, such as an earthquake shake [4]. There are many components or dimensions that have to be considered: first, technical and economic, related to the functionality of physical systems, such as lifeline systems and essential facilities; second, organizational and social, more related to the community affected by the physical systems [4]. Several studies have been carried out subsequently, with the goal to define the concept of resilience, especially in case of extreme events when the drop of functionality, or loss, is sudden [6–8].

More specifically, a resilient system should be analyzed to capture some key factors, such as assessment of failure probabilities, evaluation on consequences from failures (in terms of lives lost, damage, and economic and social consequences), and recovery costs and time to recovery (restoration to the "original" level of functionality). Many studies have recently been focused on resiliency of communities affected by natural disasters, such as Miles and Chang [30], and Chang and Shinozuka [9]. When the concept is applied to infrastructure arena, economic impacts should be defined in terms of many parameters. In particular, the losses should include both direct and indirect costs [3, 14].

The paper aims at to assess SR by considering first the probabilities of failures induced by the effects of soil–structure interaction (SSI) on several isolated bridge configurations. Second, the presented study wants to consider the damage in terms of economic consequences and, finally, to calculate recovery costs and time to reset the "original" level of functionality.

Published online: 26 January 2017

Since the Northridge earthquake, research studies have proved the significant role that soil–structure interaction (SSI) can play during seismic excitations especially on isolated bridges, as reported in Forcellini [15]. In particular, past earthquakes all over the world have proved the benefits of isolation technique for pier protection. These effects can be strongly modified by soil deformability and energy dissipation in the ground, as shown in Vlassis and Spyrakos [33], Tongaonkar and Jangid [31], Ucak and Tsopelas [32], and Forcellini [15].

The paper aims at evaluating the relationships among various characteristics of a benchmark bridge, including ground motion, superstructure, foundation, and isolation devices. The target is to assess the performance of various isolated configurations adopting a performance-based earthquake engineering (PBEE) methodology developed by the Pacific Earthquake Engineering Research (PEER) Center (http://peer.berkeley.edu). SSI effects are assessed by comparing different configurations where isolation technique is applied. Responses are assessed in terms of repair costs and time.

In this regard, past earthquakes all over the world have proved the benefits of isolation technique for pier protection. These effects can be strongly modified by soil deformability and energy dissipation in the ground, as shown in Vlassis and Spyrakos [33], Tongaonkar and Jangid [31], Ucak and Tsopelas [32], and Forcellini [14]. In the paper, SR has been assessed by considering the effects of a set of motions by considering the soil–structure interaction (SSI) on several isolated bridge configurations. In particular, the seismic response of the case study has been represented through a numerical model (Fig. 2) performed with OpenSees [29], able to couple the structure together with the foundation soil. The results have been performed with the PBEE methodology to consider the damage in terms of economic consequences and to calculate recovery costs and time to reset the original level of functionality. The novelty of the paper consists in applying these outcomes to estimate the SR of the bridge and thus proposing an attempt of application to a real case study. In particular, recovery costs and time have been implemented inside the definition of resilience by Cimellaro et al. [7]. The analytical expression of system functionality has been modelled as a linear function. Other assumptions have been made to define the loss function and the recovery function.

Case study

This paper performs a case study of an original benchmark bridge studied at the University of California [26, 28]. The benchmark bridge under investigation is intended to be representative of the prevalent ordinary construction types for California highways designed according to the

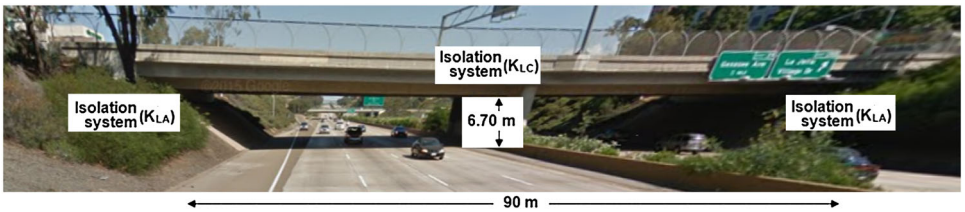

Fig. 1 Benchmark bridge

Table 1 Data models

	KL_A (kN/m)	KL_C (kN/m)	Isolation	Analytical model
I-01	1460	Fixed	Abutment isolation	Linear
I-02	1460	2920	Full isolation	Linear
I-03	NL	NL	Full isolation	Two-spring model

Table 2 Soil models

	Hard	Stiff clay	Medium clay	Soft clay
Mass density (t/m^3)	2.1	2.0	1.5	1.3
Reference shear modulus (kPa)	2.10×10^6	3.70×10^5	6.00×10^4	1.30×10^4
Reference bulk modulus (kPa)	1.05×10^7	1.85×10^6	3.00×10^5	6.80×10^4
Cohesion (kPa)	180	75	37	18
Shear wave velocity (m/s)	1000	430	200	100
Characteristic site period (s)	0.08	0.186	0.40	0.80

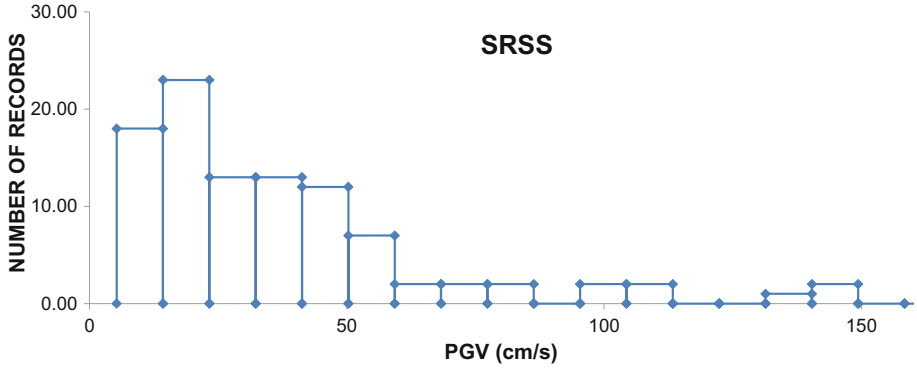

Fig. 2 NGA input motions (hystograms—SRSS of two lateral ground motion components)

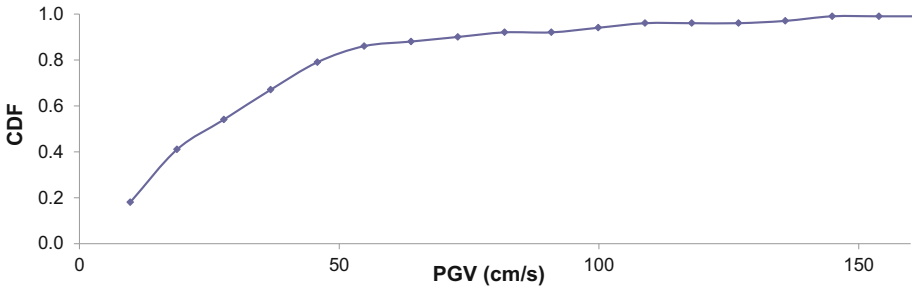

Fig. 3 NGA input motions (CDF—SRSS of two lateral ground motion components)

CALTRANS, [5] seismic design criteria and can be classified as ordinary standard bridge (OSBs). The properties were derived from the Type 1 class of bridge design [18]. The bridge is a 90 m-long, 2-span structure, supported by one circular column (1.22 m diameter), 6.70 m above grade. The deck is 11.90 m wide and 1.80 m deep and the weight is 130.30 kN/m. Each abutment is 25 m long with 30,000 kN as total weight (see Fig. 1).

The original configuration has been equipped with isolation devices, as shown in Table 1. First of all, the study considers the original model (I-01) with isolated abutments, roughly representative of a rubber bearing isolator, currently used in design. To increase bridge flexibility, the original connection between the top of the column and the deck has been removed and performed with two different types of isolators. In I-02 model, isolation is reproduced with a linear elastic behaviour representative of several bearing isolators. In I-03 model, isolators on the top of the column and on each abutment have been performed with a two-spring model [12, 16, 17] as to perform friction pendulum non-linear behaviour. SSI effects have been assessed by increasing soil deformability from a hard soil (simulating fixed conditions and consequently neglecting SSI effects) to three cohesive soils representative of stiff, medium, and soft clays, as presented in Table 2.

To reproduce typical California seismicity, the study performs 100 input motions, selected from the PEER NGA database (http://peer.berkeley.edu/nga/, [1]) and consisting of 3D input ground motions triplets. Each motion is composed of three perpendicular acceleration time history components (2 lateral and 1 vertical). Motions were divided into 5 bins of 20 motions each with characteristics: moment magnitude (M_w) 6.5–7.2 and closest distance (R) 15–30 km, M_w 6.5–7.2 and R 30–60 km, M_w 5.8–6.5 and R 15–30 km, M_w 5.8–6.5 and R 30–60 km, and M_w 5.8–7.2 and R 0–15 km. In this paper, peak ground velocity (PGV) has been considered as the most representative intensity measures (IM) and all the results have been referred to it. In particular, PGV have been calculated for each shaking direction and also for the square root-sum-of-squares (SRSS) in the two horizontal directions. Figures 2 and 3 show histograms and PGV cumulative distribution functions (CDF), respectively, and considering SRSS

Table 3 Natural periods (first and second) of the considered configurations (I-01, I-02, and I-03) in correspondence with different soil conditions (hard, stiff, medium, and soft)

Model	Hard		Stiff		Medium		Soft	
	T1 (s)	T2 (s)	T1 (s)	T2 (s)	T1 (s)	T2 (s)	T1 (s)	T2 (s)
I-01	0.811	0.506	0.809	0.505	0.893	0.510	1.020	0.800
I-02	0.843	0.690	0.855	0.694	0.880	0.719	1.000	0.800
I-03	0.813	0.527	0.866	0.527	0.926	0.529	1.130	0.805

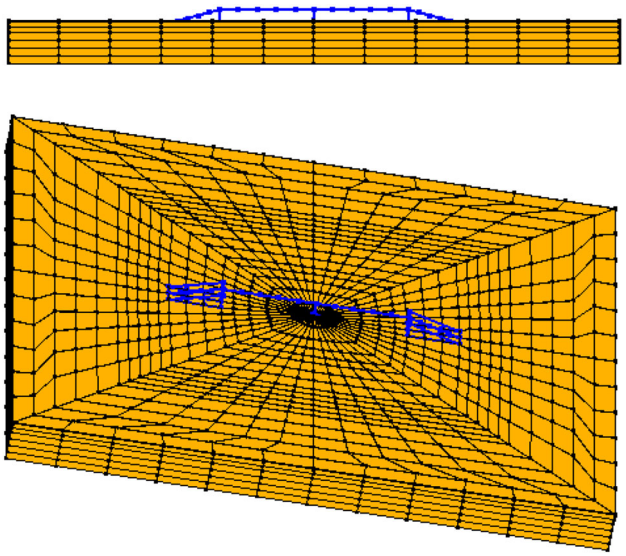

Fig. 4 Soil–structure FE model: 3D and vertical view

combination. In particular, Fig. 3 shows that the records utilized have PGV values between 0 and 160 cm/s. The period of 1 s was selected to be consistent with traditional hazard analysis as well as be close to the fundamental period of the bridge structure (Table 3). The NGA database has been chosen, because the frequencies of the input motions are close to the fundamental frequencies of the system, to affect significantly its seismic performance. Finally, ground motions were applied directly at the base of the soil mesh (without any deconvolution) (for more details, see [23, 27, 28]). The study is based on the application of a performance-based earthquake engineering (PBEE) methodology, proposed by the Pacific Earthquake Engineering Research (PEER) center. This approach is based on the definition of performance groups (PG), and consists of the association of various structural and non-structural components, using the most common repair methods. Each PG contains a collection of components that reflect global-level indicators of structural performance and that significantly contribute to repair-level decisions. The notion of a PG allows grouping several components for related repair work. Therefore, PGs are not necessarily the same as the individual load-resisting structural components. PGs damage is related to specific repair procedures and repair quantities that could be used for the estimation of cost and repair effort to return the bridge to its original level of functionality. Consequently, the platform defines discrete damage states and each of these has a subset of different repair quantities, associated to a given scenario. Once the repair quantities have been established for a given scenario (damage to different PGs), the total repair costs can be generated through a unit cost function [25, 26]. Finally, for each repair quantity, an estimate of the repair effort can be obtained through a production rate.

FEM model

The finite-element model (Fig. 4) has been built with OpenSees (open system for earthquake engineering simulation) that allows high level of advanced capabilities for modelling and analysing non-linear responses of systems using a wide range of material models, elements, and solution algorithms (for more details, see [29]). The 3D mesh (Fig. 4) aims at performing tridimensional soil–structure interaction analyses, by applying OpenSees potentialities.

Soil is modelled with a 200 × 200 m, 20 m mesh built up with 7530 modes and 6550 non-linear solid brick elements called "Bbar brick", [29]. Mesh dimensions have been determined following the suggestions indicated in Attewell and Farmer [2] and Jesmani et al. [21]. Discretization is built up with relatively small elements around the bridge and gradually larger toward the outer mesh boundaries (as shown in Fig. 4) (for more details, see [11], [13],[15] and [20]). To assess local soil effects, soil has been modelled with three clay materials called pressure independent multiyield [10, 29, 34] built up with representative parameters shown in Table 2. Characteristic site periods have been calculated by assuming a uniform and damped soil [19]. Soil has been modelled with three clay materials called pressure independent multiyield [29] built up with representative parameters shown in Table 2 (more details in [13] and [15]).

The reinforced concrete column is modelled with non-linear forced-based beam-column elements and fiber cross section, with 0.2 rad/m as the maximum curvature. The column has been settled on a single Type I caltrans pile shaft (20 m length) assumed to have cross section and reinforcement continuous with the column above and below grade. The deck is assumed to be capacity designed, so that it is able to respond in the elastic range and modelled using two-noded beam-column elements (with cross area of 5.72 m^2, transversal inertia 2.81 m^4, and vertical inertia 53.9 m^4) (more details in Forcellini [15]). The interface between the column and the soil has been modelled with rigid beam-column links, normal to the pile longitudinal axis. The soil domain 3D brick elements are connected to the column at the outer nodes of these rigid links using the equalDOF constraint in OpenSees for translations only that connects two separate points (one belonging to the structure and the second to the soil) and

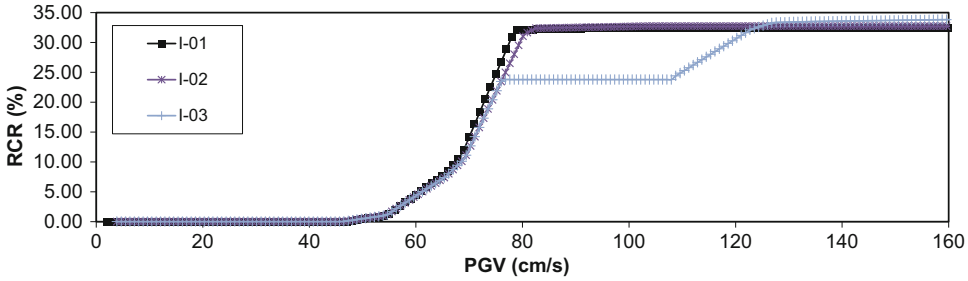

Fig. 5 total repair cost ratio (%) (hard soil)

imposes equality of displacements (for more details, see [29]). The approach ramp model connects the bridge longitudinal boundaries to the ground using a trapezoidal arrangement of rigid link elements that extends 0.5 m into the soil domain below the abutments (Fig. 4). The rigid link assembly captures the embankment and approach geometry, and permits interaction with the bridge at its ends, including the potential embankment settlement into the surrounding soil. The abutment model provides the interface between the approach ramps and the bridge ends to simulate the concrete type abutment configuration, studied in this paper. Connections between the abutments and the deck are performed with a model developed by Mackie and Stojadinovic [24] which includes sophisticated longitudinal, transverse, and vertical pads able to simulate non-linear abutment response (more details in [15]).

Finally, the bearings have been modelled in longitudinal direction only and considered very stiff in the other directions (vertical and transversal). Two types of isolation devices (elastomeric bearings and frictional/sliding bearings) are performed here, in order to represent the ones applied in many countries all over the world, as shown in [20]. Table 1 shows the studied several configurations, depending on where the devices have been placed (over the column as well as at the abutments). Isolator modelling and the applied parameters are detailed in Forcellini [15].

Resilience calculation

Resilience represents the functionality of an infrastructure system after a disaster and can be represented by time which it takes for a system to return to pre-disaster levels of performance. In particular, the previous studies have defined and calculated resilience of various lifeline systems such as [6] and [7]. Resilience is a dimensionless quantity that is able to represent the rapidity to the pre-damaged functionality level. As shown in Cimellao et al. [8], seismic resilience can be calculated as follows:

$$\mathrm{SR} = \int_{t_{0E}}^{t_{0E}+T_{\mathrm{LC}}} \frac{Q(t)}{T_{\mathrm{LC}}}\,\mathrm{d}t = \int_{0}^{\mathrm{RT}} \frac{Q(t)}{\mathrm{RT}}\,\mathrm{d}t \qquad (1)$$

where t_{0E} is here consider zero and T_{LC} is consider equal to the total repair time (RT), calculated by the PBEE methodology.

Following Cimellaro et al. [7] represents system functionality and fundamentally is built up with a loss function and a recovery function of the system performance during the system interruption. In this study the recovery function has been considered linear from Q_0 representing the reduced functionality due to the event and Q_{F} is the final functionality that has been considered equal to 100% of the original value. The main assumption of this study is that the Q_0 value has been considered proportional to the total repair costs calculated by the PBEE methodology.Therefore

$$Q(t) = \frac{1-Q_0}{\mathrm{RT}}t + Q_0 = \frac{1-\alpha\times\mathrm{RCR}}{\mathrm{RT}}t + \alpha\times\mathrm{RCR}. \qquad (2)$$

As deduced by PBEE methodology, RT and RCR are functions of an intensity measure. In this paper, PGV has been selected, and thus

$$\begin{aligned}\mathrm{SR}(\mathrm{PGV}) &= \int_{0}^{\mathrm{RT}} \frac{Q(t)}{\mathrm{RT}}\,\mathrm{d}t = \frac{\mathrm{RT}}{2}\times(1+Q_0)\\ &= \frac{\mathrm{RT}(\mathrm{PGV})}{2}\times(1+\alpha\times\mathrm{RCR}(\mathrm{PGV})).\end{aligned} \qquad (3)$$

Results

In this paragraph, the response of hard soil (Figs. 5, 6) and deformable soils (Figs. 8, 9) has been shown. The figures consider PGV as the intensity measure to reproduce the system performance. These results have been applied to the resilience notions implemented in the previous paragraph. Figures 7 and 10 show the resilience for the different configurations.

Hard soil results

Figures 5 and 6 show the results in terms of total RCR and RT, and they are mainly affected by the damage at the abutments, as shown in Forcellini [15]. I-03 model shows a

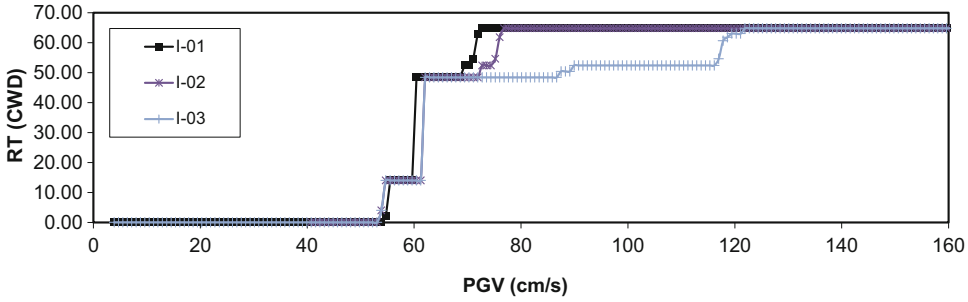

Fig. 6 Total repair time (CWD) (hard soil)

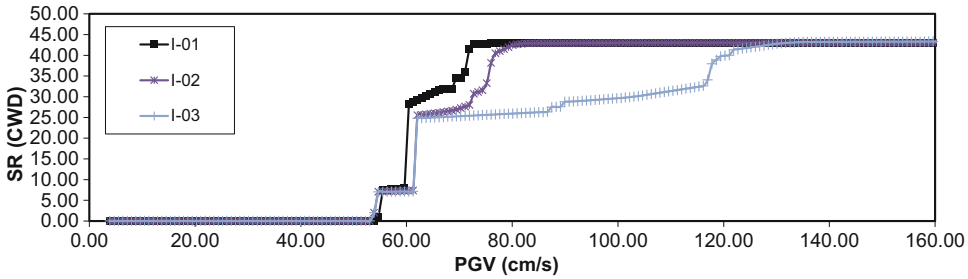

Fig. 7 Seismic resilience (CWD) (hard soil)

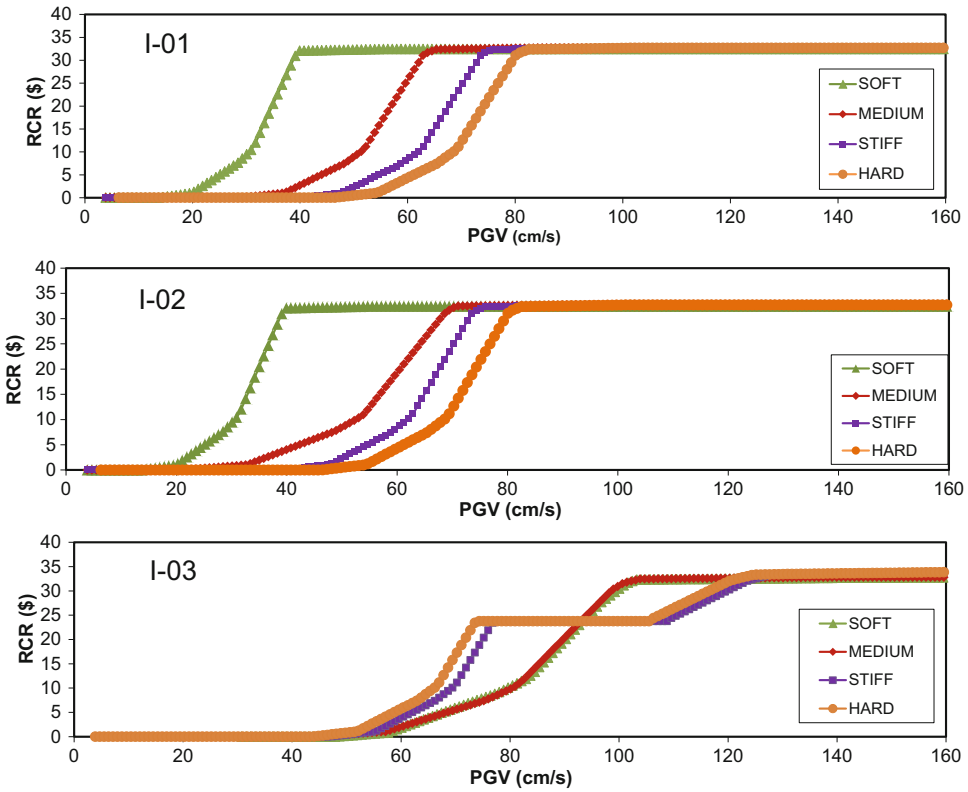

Fig. 8 Total repair cost ratio (%)

significant reduction of RCR and RT between 75 and 120 cm/s PGV values, if compared with I-02 and I-01 (linear assumptions).

Figure 7 shows that all there configurations have the same trend until PGV equal to 59.6 cm/s, after which the three curves increase (with different rates) reaching the same maximum value (SR = 42.8), at different PGV (I-01 72.7 cm/s, I-02 80.9 cm/s, I-03 120 cm/s). The differences between I-01 and I-02 are concentrated in the range: 60 and

72.7 cm/s. I-02 and I-03 differ between 72.7 and 120 cm/s. Isolation effectiveness increases with high values of PGV. In particular, the I-03 model increases slowly than I-01 and I-02. For example, in correspondence with PGV equal to 73.5 cm/s, I-02 and I-03 results are around 31.1 and 25.5, respectively, less than the values obtained for the I-01 configuration (42.8).

SSI results

Figures 8, 9 and 10 show the influence of soil deformability considering repair cost ratio (RCR), repair time (RT), and SR for the three isolated configurations.

Figures 8 and 9 show that, for I-03 on soft and medium soils, RCR and RT increase starts at higher values if compared with I-01 and I-02 configurations. In particular, in case of soft soil, the values at which damage starts increasing are, respectively, 20 cm/s for I-01 and I-02 models, while 50 cm/s for I-03 model. For stiff and hard soils, effects of non-linearity are particularly evident between 70 and 120 cm/s where RCR and RT values are lower than those in correspondence with I-01 and I-02 models. These results confirm the benefit of adopting sliding systems instead of the traditional isolators. Figures 8 and 9 show that soil affects the response in the range of PGV: 20–70 cm/s for I-01 and I-02 and 50–120 cm/s for I-03. In particular, soil deformability is detrimental to I-01 and I-02 models, since RCR and RT increase is smoother for hard soil. For I-03 model, there is a level of PGV after which RCR and RT reach the same maximum value (RCR = 35% and RT = 65 CWD). This level for soft and medium soils is around 95 cm/s, while for stiff and hard ones, it is around 120 cm/s. These values can be considered the points where soil deformability starts to become comparable with the shear strain imposed during seismic excitation and thus the influence of column damage starts to affect RCR and RT. In this regard, the damage can be reduced only increasing soil stiffness (for example with deep foundations or soil improvement). RCR equal to 35% and RT equal to 68 CWD are reached for all the configurations (at different levels of PGV), no manner which soil has been considered.

Figure 10 shows that every configuration reaches the same max value (equal to 37.5). I-01 and I-02 trends are similar for all the considered soils. Soil deformability is detrimental, since the PGV value at which SR starts increasing becomes smaller when soil deformability increases. For I-03 soft and medium soils, trends are close each other. The same happens for stiff and hard ones. Between the range of PGV 53.1 and 81.7 cm/s, SR for stiff and hard soil is bigger than soft and medium ones (soil deformability is conservative). On the contrary, between

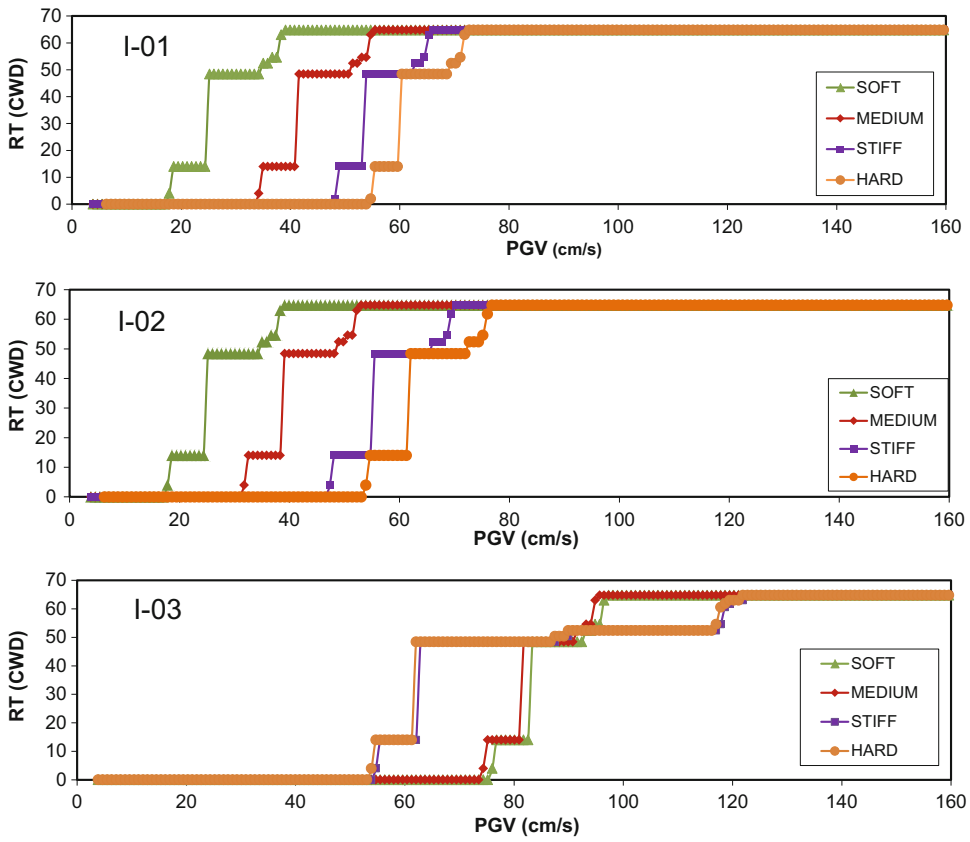

Fig. 9 Total repair time (CWD)

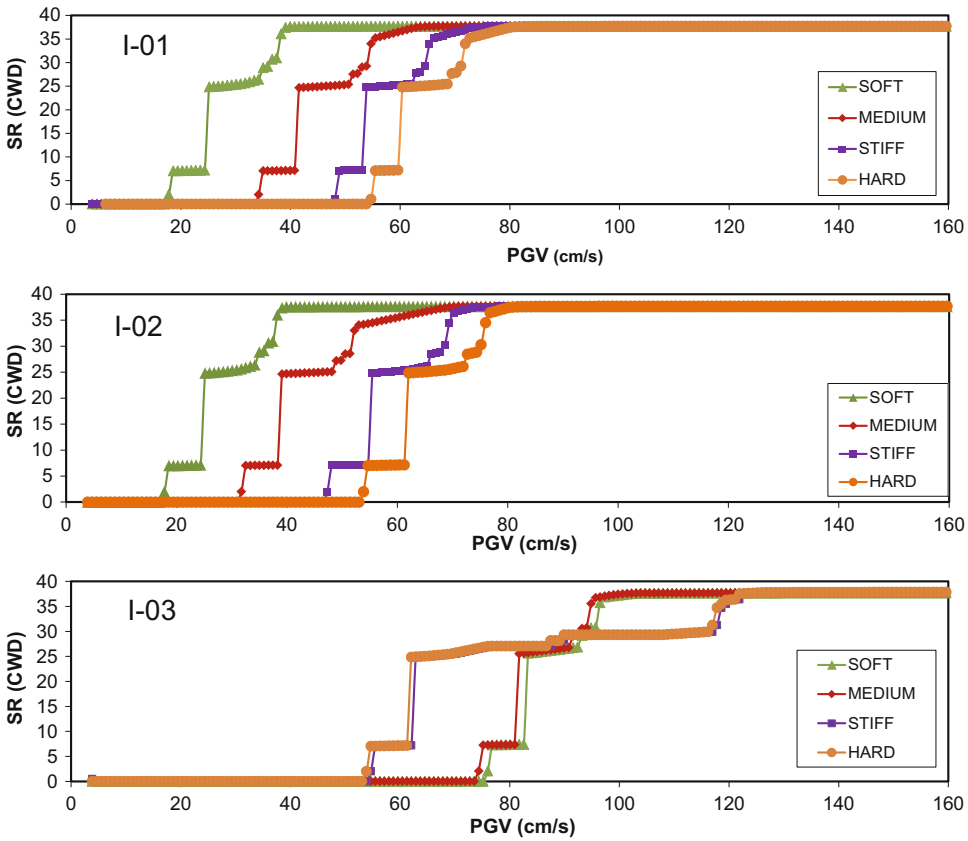

Fig. 10 Seismic resilience

PGV 94.9 and 121 cm/s, soil deformability is shown to be detrimental. In particular, For I-03 model, the level of PGV after which SR reaches the same maximum value (37.5) for soft and medium soils is around 95 cm/s, while for stiff and hard ones, it is around 120 cm/s.

Conclusions

The study conducted in this paper may be viewed as an original contribution to the assessment of SR of a benchmark bridge taking into consideration economic performance in terms of repair costs and time. In particular, SSI effects have been assessed by comparing different configurations where isolation technique is applied. The mutual effect of soil and isolations properties has been studied to assess the best isolated configuration able to fit the different non-linear conditions of the soil, by applying a PBEE approach. The resilience of the structure has been calculated by applying the classical formulation with some assumptions regarding the recovery functions. This formulation is able to include the performance quantities deduced by PBEE methodology (RT and RCR) that are functions of a selected intensity measure (PGV in the paper). The formulation is general and the paper can be considered a first application of such formulation to the specific case of the presented benchmark bridge. Further analysis will aim to reproduce more cases of bridges and to develop the formulation with more sophisticated parameters and assumptions.

References

1. NGA database. http://peer.berkeley.edu/nga/. Accessed 20 Nov 2016
2. Attewell P, Farmer IW (1973) Attenuation of ground vibrations from pile driving. Ground Eng 6(4):26–29
3. Brookshire DS, Chang SE, Cochrane H, Olson RA, Rose A, Steenson J (1997) Direct and indirect economic losses from earthquake damage. Earthq Spectra 14(4):683–701
4. Bruneau M, Chang S, Eguchi R, Lee G, O'Rourke T, Reinhorn AM, Shinozuka M, Tierney K, Wallace W, Winterfelt D (2003) A framework to quantitatively assess and enhance the seismic resilience of communities. Earthq Spectra 19(4):733–752
5. CALTRANS (1994) The Ndhridge earthquake. Post Earthquake Investigation Report
6. Cimellaro GP, Fumo C, Reinhorn AM, Bruneau M (2009) Quantification of seismic resilience of health care facilities. MCEER Technical Report-MCEER-09-0009. Multidisciplinary Center for Earthquake Engineering Research, Buffalo
7. Cimellaro GP, Reinhorn AM, Bruneau M (2010) Seismic resilience of a hospital system. Struct Infrastruct Eng 6(1–2):127–144

8. Cimellaro GP, Reinhorn AM, Bruneau M (2010) Framework for analytical quantification of disaster resilience. Eng Struct. doi:10.1016/j.engstruct.2010.08.008 **(in press)**
9. Chang SE, Shinozuka M (2004) Measuring improvements in the disaster resilience of communities. Earthq Spectra 20(2):739–755
10. Elgamal A, Yang Z, Parra E, Ragheb A (2003) Modeling of cyclic mobility in saturated cohesionless soils. Int J Plast 9(6):883–905
11. Elgamal A, Lu J, Forcellini D (2009) Mitigation of liquefaction-induced lateral deformation in sloping stratum: three-dimensional numerical simulation. J Geotech Geoenviron Eng 135(11):1672–1682
12. Forcellini D, Kelly JM (2014) The analysis of the large deformation stability of elastomeric bearings. J Eng Mech ASCE. doi:10.1061/(ASCE)EM.1943-7889.0000729
13. Forcellini D, Gobbi S (2015) Soil structure interaction assessment with advanced numerical simulations. In: Computational Methods in Structural Dynamics and Earthquake Engineering (COMPDYN) conference, Crete Island, 25–27 May 2015
14. Forcellini D (2016) A direct-indirect cost decision making assessment methodology for seismic isolation on bridges. J Math Syst Sci 4(03–04):85–95. doi:10.17265/2328-224X/2015.0304.002
15. Forcellini D (2017) Cost assessment of isolation technique applied to a benchmark bridge with soil structure interaction. Bull Earthq Eng 15:51. doi:10.1007/s10518-016-9953-0
16. Kelly JM (1997) Earthquake-resistant design with rubber, 2nd edn. Springer, London
17. Kelly JM (2003) Tension buckling in multilayer elastomeric bearings. J Eng Mech ASCE 129(12):1363–1368
18. Ketchum M, Chang V, Shantz T (2004) Influence of design ground motion level on highway bridge costs. Report no. Lifelines 6D01, Pacific Earthquake Engineering Research Center, Berkeley
19. Kramer SL (1996) Geotechnical earthquake engineering. Prentice Hall, Inc., Upper Saddle River, New Jersey, p 653
20. Kunde MC, Jangid RS (2003) Seismic behavior of isolated bridges: a state-of the art review. Electron J Struct Eng 3(2):140–170
21. Jesmani M, Fallahi AM, Kashani HF (2012) Effects of geometrical properties of rectangular trenches intended for passive isolation is sandy soils. Earth Sci Res 1(2):137–151
22. Lu J, Mackie KR, Elgamal A (2011) BridgePBEE: OpenSees 3D pushover and earthquake analysis of single-column 2-span bridges, user manual, Beta 1.0. http://peer.berkeley.edu/bridgepbee/. Accessed 20 Oct 2016
23. Mackie KR, Stojadinovic B (2006) Fourway: a graphical tool for performance-based earthquake engineering. J Struct Eng 132(8):1274–1283
24. Mackie KR, Wong J-M, Stojadinovic B (2008) Integrated probabilistic performance-based evaluation of benchmark reinforced concrete bridges. PEER Center, University of California, Berkeley Report No. 2007:09
25. Mackie KR, Wong J-M, Stojadinovic B (2010) Post-earthquake bridge repair cost and repair time estimation methodology. Earthq Eng Struct Dyn 39(3):281–301
26. Mackie KR, Lu J, Elgamal A (2010) User interface for performance-based earthquake engineering: a single bent bridge pilot investigation. In: 9th US National and 10th Canadian conference on earthquake engineering: reaching beyond borders. July 25–29, Toronto
27. Mackie K, Lu J, Elgamal A (2012) Performance-based earthquake performance-based earthquake assessment of bridge systems including ground-foundation interaction. Soil Dyn Earthq Eng 2(2012):184–196
28. Mazzoni S, McKenna F, Scott MH, Fenves GL et al (2009) Open system for earthquake engineering simulation, user command-language manual. Pacific Earthquake Engineering Research Center, University of California, Berkeley, OpenSees version 2.0. http://opensees.berkeley.edu/OpenSees/manuals/usermanual
29. Miles SB, Chang SE (2003) Urban disaster recovery: a framework and simulation model. MCEER-07-0014 (PB2004-104388, A07, CD-A07)
30. Tongaonkar NP, Jangid RS (2003) Seismic response of isolated bridges with soil-structure interaction. Soil Dyn Earthq Eng 23(4):287–302
31. Ucak A, Tsopelas P (2008) Effect of soil-structure interaction on seismic isolated bridges. J Struct Eng 134(7):1154–1164
32. Vlassis AG, Spyrakos CC (2001) Seismically isolated bridge piers on shallow soil stratum with soil-structure interaction. Comput Struct 79(32):2847–2861
33. Yang Z, Elgamal A, Parra E (2003) A computational model for cyclic mobility and associated shear deformation. J Geotech Geoenviron Eng (ASCE) 129(12):1119–1127